Exp.-Nr. A2/ 5/05
Eingang: 26.08.05
an PAC:

Mainz Microtron MAMI

Collaboration A2: "Real Photon Experiments"
Spokesperson: A. Thomas

Proposal for an Experiment

Recoil nucleon polarimetry observables in meson photoproduction at MAMI

Collaborators :
CrystalBall@MAMI collaboration

Spokespersons for the Experiment :
D.P. Watts - University of Edinburgh
G. Rosner, D.I Glazier - University of Glasgow
P. Pedroni - INFN, Pavia

Abstract of Physics :
We will develop a nucleon polarimetry capability for use in measurements with the Crystal Ball (CB) and TAPS detector systems at MAMI. Employment of this new facility with the existing polarised photon beam will allow detailed measurement of the double-polarisation observables $C_{x'}$ (circularly polarised photons + recoil polarisation), $O_{x'}$ (linearly polarised photons + recoil polarisation) and the single polarisation observables P (recoil asymmetry) and T (target asymmetry) for both π^0 and η production. Many of these observables will be measured for the first time giving new constraints on the contributing mechanisms and nucleon resonances in meson photoproduction.

Abstract of Equipment :
The tagged photon spectrometer will be used with the MAMI beam at 0.85 and 1.5 GeV. The CB and TAPS detectors will be used to detect photons from π^0 and η decays. The nucleon polarimeter will require a $\sim$ 7cm thick graphite scatterer to be placed at the downstream exit of the CB.

MAMI–Specifications :

beam energy	885 MeV and 1500 MeV
beam current	$<$ 100 nA
time structure	cw
polarization	none

Experiment–Specifications :

experimental hall/beam	A2
detector	Crystal Ball and TAPS as forward wall
target material	Liquid Hydrogen

Beam Time Request :

set–up without beam	($\approx$ 3 weeks)
set–up/tests with beam	100 hours
data taking	300 hours at 885 MeV and 500 hrs at 1500 MeV

Title: **Recoil nucleon polarimetry observables in meson photoproduction at MAMI**

Participants: J. Brudvik, J. Goetz, B.M.K. Nefkens, S.N. Prakhov, A. Starostin, and I. Suarez, **University of California, Los Angeles, CA, USA**

J. Ahrens, H.J. Arends, D. Drechsel, D. Krambrich, M. Rost, S. Scherer, A. Thomas, L. Tiator, D. von Harrach and Th. Walcher, **Institut für Kernphysik, University of Mainz, Germany**

R. Beck, M. Lang, A. Nikolaev, S. Schumann, and M. Unverzagt, **Helmholtz–Institut für Strahlen- und Kernphysik, Universtät Bonn, Germany**

S. Altieri, A. Braghieri, P. Pedroni, and T. Pinelli, **INFN Sezione di Pavia, Pavia, Italy**

J.R.M. Annand, R. Codling, E. Downie, D.I. Glazier, J. Kellie, K. Livingston, J.C. McGeorge, I.J.D. MacGregor, R.O. Owens, D. Protopopescu, G. Rosner, **Department of Physics and Astronomy, University of Glasgow, Glasgow, UK**

C. Bennhold and W. Briscoe, **George Washington University, Washington, USA**

S. Cherepnya, L. Fil'kov, and V. Kashevarow, **Lebedev Physical Institute, Moscow, Ru ssia**

V. Bekrenev, S. Kruglov, A. Koulbardis, and N. Kozlenko, **Petersburg Nuclear Physics Institute, Gatchina, Russia**

B. Boillat, B. Krusche and F. Zehr, **Institut für Physik University of Basel, Base l, Ch**

P. Drexler, F. Hjelm, M. Kotulla, K. Makonyi, V. Metag, R. Novotny, M. Thiel, and D. Trnka, **II. Physikalisches Institut, University of Giessen, German y**

D. Branford, K. Foehl, C.M. Tarbert and D.P. Watts, **School of Physics, University o f Edinburgh, Edinburgh, UK**

V. Lisin, R. Kondratiev and A. Polonski, **Institute for Nuclear Research, Moscow, Russia**

J.W. Price, **California State University, Dominguez Hills, CA, USA**

D. Hornidge, **Mount Allison University, Sackville, Canada**

P. Grabmayr and T. Hehl, **Physikalisches Institut Universität Tübingen, Tübingen, Germany**

Yu.A. Usov, and S.B. Gerasimov, **JINR, Dubna, Russia**

H. Staudenmaier, **Universität Karlsruhe, Karlsruhe, Germany**

D.M. Manley, **Kent State University, Kent, USA**

M. Korolija and I. Supek, **Rudjer Boskovic Institute, Zagreb, Croatia**

D. Sober, **Catholic University, Washington DC**

M. Vanderhaeghen, **College of Williams and Mary, Williamsburg, USA**

Spokespersons: D.P. Watts, Univ. of Edinburgh (daniel.watts@ph.ed.ac.uk tel: +44 131 650 5286)
G. Rosner, D.I Glazier, Univ. of Glasgow
P. Pedroni, INFN, Pavia

1 Abstract of Physics

We will develop a nucleon polarimetry capability for use in measurements with the Crystal Ball and TAPS detector systems at MAMI. Employment of this new facility with the existing polarised photon beam will allow detailed measurement of the double-polarisation observables $C_{x'}$ (circularly polarised photons + recoil polarisation), $O_{x'}$ (linearly polarised photons + recoil polarisation) and the single polarisation observables P (recoil asymmetry) and T (target asymmetry) for both π^0 and η production. The T observable is accessed from the y component of transferred recoil polarisation with linearly polarised photons. Many of these observables will be measured for the first time, giving new constraints on the contributing mechanisms and nucleon resonances in meson photoproduction.

1.1 Scientific case.

1.1.1 Introduction

Detailed knowledge of the spectrum of nucleon resonances and determination of their their mass, lifetime, quantum numbers and couplings give important constraints on models of nucleon structure. Due to the short lifetimes of the nucleon resonances they tend to overlap and this unfavourable situation has led to serious ambiguities in our knowledge of the resonance spectrum, even after decades of study. This is a serious shortcoming in attempts to learn about how quarks interact to form nucleons.

Comparison of the fundamental nucleon resonance spectrum with theoretical models should in principle help to establish the appropriate dynamics and degrees of freedom in the nucleon. Constituent quark models have been widely used to give predictions of the spectrum of nucleon resonances. However a large number of resonances that appear in the symmetric constituent quark models have not yet been observed and it is not established if these states do not exist, or simply have not given sufficiently strong signals in the presently available experimental data. This makes it difficult to separate even very basic dynamical models about how the constituent quarks interact in the nucleon. In the next decade significant progress is expected in less phenomenological theoretical descriptions of the nucleon resonance spectrum. In particular calculations directly from QCD using Lattice techniques are starting to give predictions for the low-lying nucleon resonances. For example, a recent lattice calculation predicts masses of the lowest states of octet and decuplet baryons and clearly shows the the $1/2^+(1440)$ Roper state as the first T=1/2 excited state of the nucleon for the first time[1]. Also, there is the possibility of chiral symmetry restoration exhibited by the high lying and poorly established states[2]. Recently predictions of the nucleon spectrum have also been developed which are based on a holographic dual of QCD[3]. In light of the theoretical advances already made, and their expected development in future years, it is timely to firm up our knowledge of this fundamental spectrum.

One direction taken to address this problem is to explore if different sensitivities to the nucleon excitation spectrum can be obtained in measurement of higher mass meson production reactions such as η, η', ω, ρ and strangeness production such as $K\Lambda$ and $K\Sigma$. Measurements of this type are presently a major activity at many of the world's photon and electron beam facilities and evidence for some missing resonances has been presented in recent years.

However, it is important to note that even for the most widely studied and simpler π photoproduction reaction the world's experimental data is not yet comprehensive. The photoproduction of pseudo-scalar mesons from the nucleon can be described theoretically by 4 helicity amplitudes, which lead to 16 real experimental observables. To fully pin down these amplitudes without model ambiguities requires the measurement of at least 8 observables which makes necessary the measurement of cross sections, single polarisation and double-polarisation observables. There has been significant experimental effort to determine these polarisation observables to better constrain the nucleon resonance spectrum. In particular recent years have seen a lot of experimental

activity towards determining double-polarisation observables where the polarisation of two of either beam, target and recoiling nucleon are determined in the experiment. Each measurement of a double-polarisation observable gives information on a different bi-linear combination of the helicity amplitudes. Due to the relationships between the double-polarisation observables, measurements with recoil polarisation are absolutely necessary to pin down the amplitudes unambiguously. An example of the effectiveness of double-polarisation observables with recoil polarisation is seen in Ref.[5] where $C_{x'}$ measurements are predicted to be particularly effective in revealing some of the missing or poorly established resonances.

Major programmes to measure beam-target double polarisation observables are in place at many of the leading photon and electron beam facilities to improve the constraints on meson production. These new data have shown their worth. For example recent measurements highlight the need for revised photocouplings for even "well established" resonances such as the $D_{13}(1520)$[4]. With the proposed development of a recoil polarimeter we will access the double polarisation observables $C_{x'}$ (circularly polarised photon beam + recoil) and $O_{x'}$ (Linearly polarised photon beam + recoil) in both π and η photoproduction. All these measurements will either be the first determination of the observable or comprise the first detailed measurement of the observable in the energy range of MAMI-C. The data will be complementary to the beam-target measurement programmes at MAMI and other laboratories. The propsals A2/**** and A2/*** submitted to this PAC will determine the beam+target double polarisation observables E and G in similar kinematics to the proposed measurement. Combining the results will give the 8 observables necessary to fully constrain the helicity amplitudes.

1.2 Previous experiments

1.2.1 π^0 photoproduction

The world's $p(\gamma,p)\pi^0$ data for the observables accessible in the proposed experiment are shown in Fig. 1. The data taken at all breakup angles are included. It is clear that there is a reasonable number of measurements of the single polarisation observables P and T, mainly obtained in the 70's and 80's. These data will be a useful cross check of our experiment and we will add new high quality data to the data base.

The experimental situation is significantly worse for the double-polarisation data. There have been some pioneering measuerements of $O_{x'}$ at Kharkov and Yerevan, but the statistical accuracy and kinematic coverage is rather poor. Although not yet in the SAID database (and therefore not on Fig.1) there is a recent measurement of $C_{x'}$ (circular polarised photon beam + recoil) in an experiment published in 2002 by the Hall A collaboration at Jefferson Lab[6]. The $p(\gamma,p)\pi^0$ reaction was isolated from the interaction of an untagged photon beam with the target by accurate determination of the proton energy and angle in a magnetic spectrometer . The observables $C_{x'}$, $C_{z'}$ and P were measured at 6 photon energies in the range 0.8 – 4 GeV. The data were taken mainly at high photon energies to look for signals for the onset of a perturbative QCD regime. The sparse data in the region accessible at MAMI-C was not well described by the present partial wave analyses of the world's pion photoproduction data, which even predicts the wrong sign in certain kinematic regions, highlighting how double polarisation observables give new sensitivity.

1.2.2 η photoproduction

There are no published measurements of any double-polarisation observable for η photoproduction. The single polarisation target observable has been measured recently at ELSA[7] and the linear polarisation observable Σ has been observed at GRAAL[8].

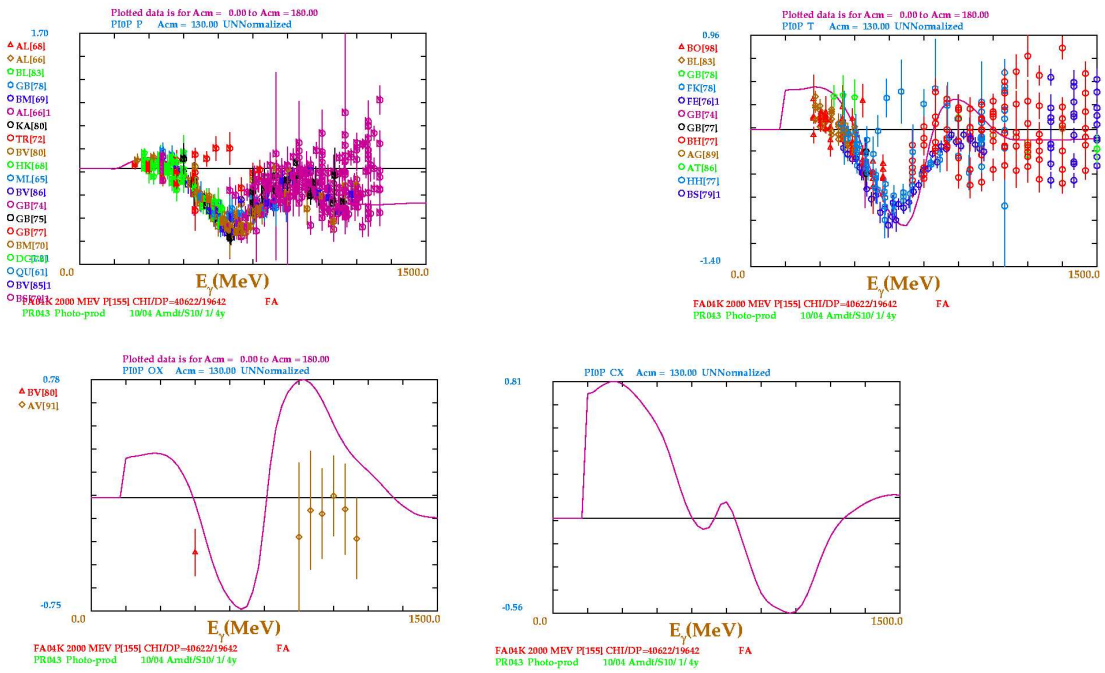

Figure 1: World's experimental data at all CM breakup angles. Clockwise from top left are shown P, T, $O_{x'}$ and $C_{x,}$ as a function of E_γ from the SAID database. The line shows the SAID predictions at a CM breakup angle of 135^0. (The recent $C_{x'}$ data[6] is not yet entered in the database)

2 Predictions of sensitivity

We have obtained predictions from the MAID and SAID parameterisations of the world's presently available data on pion photoproduction. Fig. 2 shows the predictions of MAID and SAID for a backward CM breakup angle where there will be acceptance in the proposed experiment. Predictions for all observables we can access from the experimental data are shown. Even at low E_γ where the resonance spectrum is likely to be better established MAID and SAID show different predictions, particularly for the $O_{x'}$ observable.

The MAID predictions are also shown with various resonances switched off in the calculation to get some indication of which resonances each variable is sensitive to. Various different resonances produce strong effects in our E_γ range but most markedly the $F_{15}(1680)$ shows up strongly in $C_{x'}$ around E_γ=1 GeV and the Roper resonance produces large effects on $O_{x'}$, particularly for E_γ=300-700 MeV. This sensitivity to the Roper is also illustrated in Fig. 3 where the angular distribution of $O_{x'}$ at a fixed photon energy is presented. The largest sensitivity is observed at backward CM breakup angles, where also a large sensitivity is seen in P and T.

3 Experimental aspects

The measurement will use the Crystal Ball and TAPS detector system (CBTAPS) with the Glasgow tagged photon specrometer at MAMI. The upgraded tagging facility at MAMI-C will tag bremsstrahlung photons in the energy range ~70 – 1400 MeV with a resolution of ~ 4 MeV for beam energy of 1500 MeV and with total rates of up to 10^8 s^{-1}.

The CB is constructed of 672 optically isolated NaI(Tl) crystals, 15.7 radiation lengths thick. The

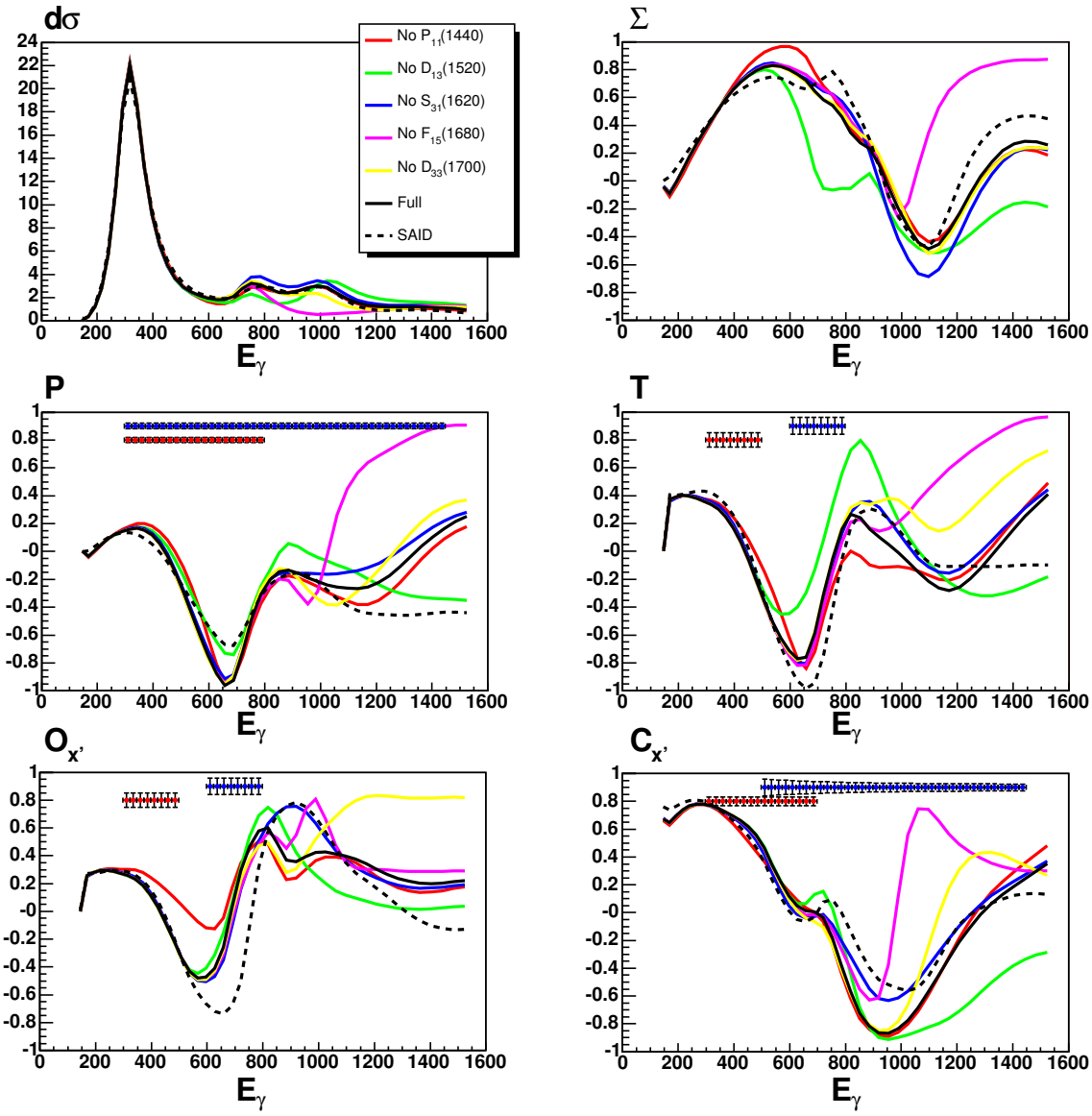

Figure 2: MAID predictions for observables accessible in the proposed measurement. The different coloured lines indicate the predictions with various resonances removed (indicated in the figure). All predictions are for a CM π^0 breakup angle of 130°. The data points show the expected statistical accuracy of the proposed measurement for the first 0.85 GeV beamtime (red) and with the 1.5 GeV beamtime (blue)

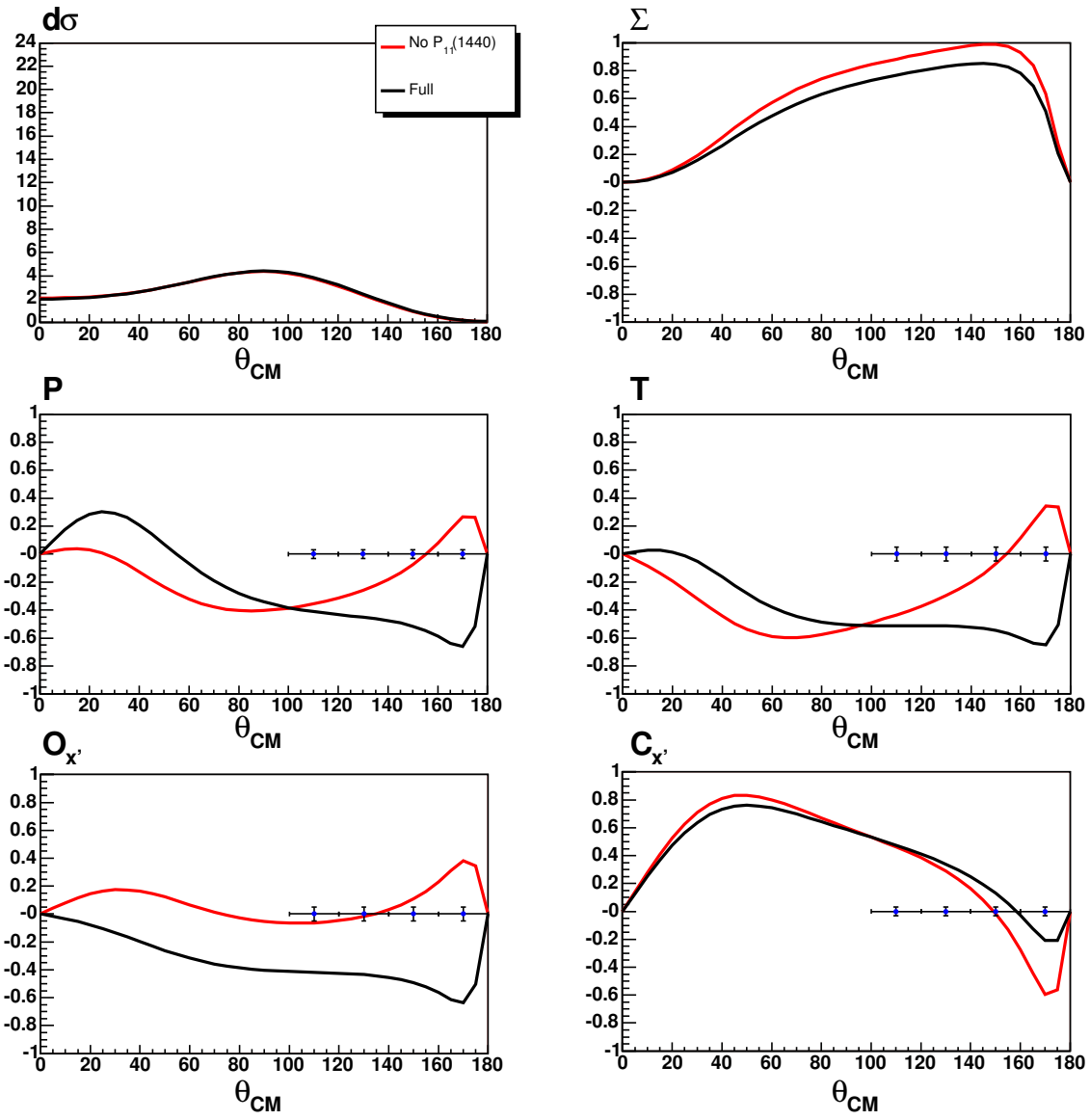

Figure 3: MAID predictions showing observables accessible in the proposed measurement at a fixed photon energy as a function of CM breakup angle. The full MAID calculation is compared to the MAID prediction with the Roper removed. The expected statistical accuracy of the measurement is indicated by the data points in the figure

detectors are arranged in a spherical shell with an inner radius of 25.3 cm and an outer radius of 66.0 cm. Each crystal is shaped like a truncated triangular pyramid, 40.6 cm high, pointing towards the center of the Ball. The sides on the inner end are 5.1 cm long and 12.7 cm at the far end. The Ball has an entrance and exit opening for the beam which results in a loss of 4.4% of acceptance. A charged particle tracker, comprised of two coaxial cylindrical multiwire proportional chambers (MWPC) similar to those used with the DAPHNE large-acceptance tracking detector [10] will be constructed for use with the Crystal Ball at MAMI-C. A plastic scintillator particle-identification detector (PID)[11] will be placed between the wire chamber and the target to separate different charged particle species.

The TAPS detector system which will cover the exit (downstream) opening of the Crystal Ball. TAPS[12] is comprised of 384 individual barium fluoride (BaF_2) crystals. The crystals are hexagonally shaped with an inscribed diameter of 59 mm and a length of 250 mm (12 radiation lengths). BaF_2 has three scintillation components in the UV region, two fast ones and a slow one. The relative light yield depends on the ionization density and, therefore, allows particle discrimination by pulse-shape analysis. The fast component provides excellent timing characteristics. In front of each TAPS detector is mounted a hexagonal plastic scintillator (NE102A) slice which is read by a separate photomultiplier. This tile acts as the "VETO" for charged events.

3.1 The nucleon polarimeter

The principle of operation of a nucleon polarimeter is based upon the coupling of angular momentum and spin of a nucleon in the scattering process from a nucleus. There is an asymmetry in the scattering direction dependent on the direction of the nucleon spin. More specifically

$$n(\theta,\phi) = n_0(\theta,\phi)\{1 + A(\theta)[P_y cos(\phi) - P_x sin(\phi)] \quad (1)$$

where n_o is the distribution for unpolarised nucleons and $A(\theta)$ is the analysing power of the scatterer. The analysing powers are generally extracted from experiment rather than theory and depend on the type of nuclei in the scattering medium. Previous polarimeters have used graphite and registered nucleon scatters in the region of 10-30 degrees, as the analysing power is well established (to within $\sim$4%) in this region.

The polarimeter design exploits the existing detector systems and is shown schematically in figure 4. The exit hole of the Crystal Ball will be covered by a graphite slab of thickness $\sim$7cm. This is chosen as a compromise between having sufficient scattering material without causing a prohibitively high energy threshold for charged particles to pass through the analyser. As graphite would be an inactive scatterer (ie. will not produce a hit signal) we will also employ thin plastic scintillator detectors over the upstream face of the graphite to give an extra check that protons entering the graphite have entry points consistent with that expected from the $p(\gamma,N)\pi$ or $p(\gamma,N)\eta$ kinematics. The highly segmented TAPS detector will detect the recoiling nucleons following their passage through the analyser material, determining their scattering angle and enabling the selection of a sufficiently clean sample of nuclear scattered events as shown below.

A GEANT simulation of the response of this polarimeter to recoiling protons from $p(\gamma,p)\pi^\circ$ has been developed. Simulated events were retained for analysis if i) there was a single hit cluster in the TAPS detector and ii) there were two neutral hit clusters produced in the Crystal Ball from which the calculated invariant mass was within 20 MeV of the accepted π^0 mass. Photon hits in TAPS were not analysed and rejected by a time-of-flight cut. Figure 6 shows the opening angle between the kinematically reconstructed proton 4-vector (calculated from the incident photon and the detected pion 4-vectors) and the proton hit in TAPS. Without the graphite in place (red line) this spectrum simply reflects the uncertainties in the calculated variable arising from i) the π detection resolution in the Crystal Ball ii) uncertainties in the target vertex position iii) uncertainty in the determination of the beam energy and iv) uncertainty in the TAPS hit position. It can

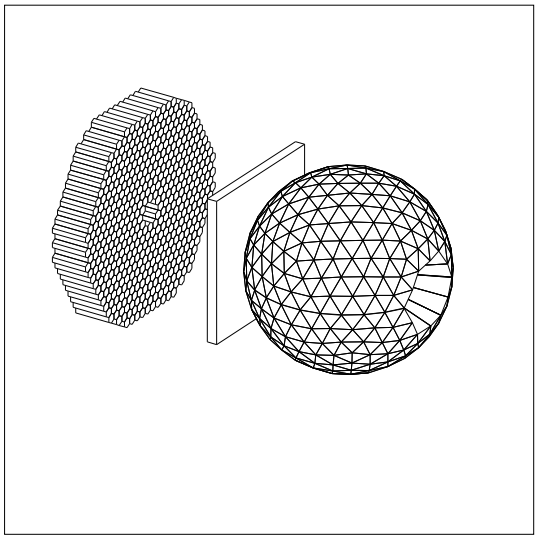

Figure 4: Schematic of the Crystal Ball and TAPS showing the graphite analyser in place over the Crystal Ball exit region

be seen that the all these factors produce an angular resolution of approx $\sigma = 3°$. The GEANT predictions when the 7cm thick graphite slab is included in the simulation are shown by the blue line. In this case the dominant peak near zero is broadened slightly, due to effects from multiple coulomb scattering of protons as they pass through the graphite. As well as the peak there is now significant strength out to wider angles arising from nuclear scattering events, and these are well separated from the coulomb scattered events for angles larger than $\sim$10°. The modelling of the low energy nucleon-nucleus interactions in GEANT is not detailed but should give a general indication of the polarimeter properties (the results were obtained with the GEANT-FLUKA package). The GEANT predictions indicate that $\sim$4% of incident nucleons are scattered between 10 - 30 degrees. This figure is similar to that realised with other graphite based nucleon polarimeters of comparable thickness, e.g. focal plane polarimeters at A1 at MAMI and in Hall A at Jefferson Lab[13].

Also shown in Fig. 6 are the GEANT predictions for the same number of initial $p(\gamma, p)\pi^0\pi^0$ events (a uniform matrix element is assumed). This reaction is likely to give the largest background. With the same cuts as described above for the single π data this background is predicted to contribute less than 0.5% in the useful angular region of the polarimeter.

The GEANT simulations give strong indications that the polarimeter will obtain a clean sample of nuclear scattered events. It will be important to obtain experimental data to prove the operation and efficiency of the polarimeter and to do this we require a test beam time of $\sim$100 hours as discussed in section 4.

3.1.1 Polarimeter acceptance

The polarimeter will have acceptance for forward angle recoiling nucleons. With the target at the centre of the Crystal Ball the acceptance will be $\sim \pm 20°$. We will position the target forward of the central position by 5cm to increase this to $\sim \pm 30°$. The kinematic sampling of the π and η photoproduction reactions by the polarimeter is illustrated in Figure 5 where plots of the CM breakup angle of the meson versus the lab angle of the recoil are presented for a range of incident photon energies. For π^0 production we will mainly sample more backward CM meson angles. For η production near threshold we will sample the reactions at all CM meson angles.

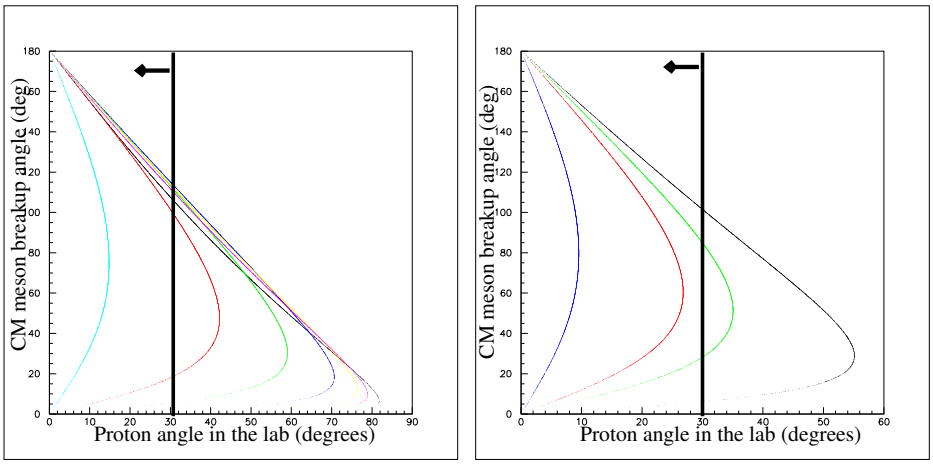

Figure 5: Left panel: Kinematics for π^0 photoproduction from the proton. The meson angle in the CM (y axis) is plotted versus the recoiling proton angle in the lab frame (x axis). The loci for E_γ = 150, 200, 300, 500, 750, 1000 and 1500 MeV are shown by the turqoise, red, green, blue, yellow, purple and black lines respectively. Right panel: Kinematics for η photoproduction from the proton. The loci for E_γ= 720, 820, 920 and 1500 MeV are shown by the blue, red, green and black lines respectively.

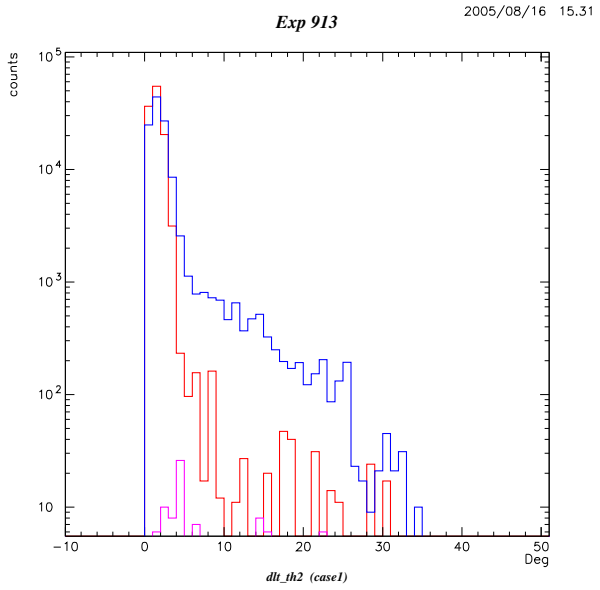

Figure 6: GEANT simulation of the $p(\gamma,p)\pi^0$ reaction at E_γ=0.5 GeV. The plot shows the angle between the proton 4-vector calculated from the incident photon energy and the pion 4-vector and the proton 4-vector calculated from the TAPS hit. The red line shows the results with no graphite analyser in place and the blue line shows the case when the analyser is in position. The predictions for the same number of initial $p(\gamma,p)\pi^0\pi^0$ is shown by the purple line

3.2 Extraction of polarisation observables

The differential cross section and recoil polarisation for pseudoscalar photoproduction, with a polarised photon beam, can be expressed as:

$$\begin{aligned}\rho_f \frac{d\sigma}{d\Omega} &= \frac{d\sigma}{d\Omega_0}[\,1 - P_\gamma^{lin}\Sigma\cos 2\phi_m + \sigma_{x'}\left(P_\gamma^{circ}C_{x'} + P_\gamma^{lin}O_{x'}\sin 2\phi_m\right) \\ &\quad + \sigma_{y'}\left(P - P_\gamma^{lin}T\cos 2\phi_m\right) + \sigma_{z'}\left(P_\gamma^{circ}C_{z'} + P_\gamma^{lin}O_{z'}\sin 2\phi_m\right)\,] \end{aligned} \quad (2)$$

where, P_γ^{lin} and P_γ^{circ} are the linear and circular polarisation of the beam; ϕ_m is the azimuthal angle of the meson in the lab. frame; and the matrices, $\sigma_{x',y',z'}$ refer to the proton quantisation axes defined by:

$$\widehat{z'} = \widehat{p}_p \quad \widehat{y'} = \frac{p_\gamma \times p_m}{|p_\gamma \times p_m|} \quad \widehat{x'} = \widehat{y'} \times \widehat{z'}$$

with p_γ, p_p and p_m being the momentum of the beam, recoil proton and meson respectively.

The Σ, P, T, $O_{x'}$ and $C_{x'}$ observables will be simultaneously extracted from the experimental data in the proposed measurement. As the nucleon polarimeter only measures transverse components of polarisation the measurement of $O_{z'}$ and $C_{z'}$ would require the precession of the proton spin in a magnetic field before the polarimeter and is outwith this proposal.

The beam asymmetry Σ is measured with a linearly polarised beam having a known degree of polarisation (P_γ^{lin}) . The resulting asymmetry in the meson azimuthal distribution, $N(\phi_m)$, can be fitted with a $\sin(2\phi_m)$ function, the amplitude of which is equal to the product $P_\gamma^{lin}\Sigma$.

The P, T, $O_{x'}$ and $C_{x'}$ require information from the nucleon polarimeter. Summing the different photon beam polarisations to give an effective unpolarised beam will allow us to access the single polarisation observable P. Denoting the scattered proton azimuthal angle as ϕ_p', the product of the polarimeter analysing power and induced nucleon polarisation, AP, can be extracted from the amplitude of a $\cos\phi_p'$ fit to the azimuthal angular distribution (the x-component of nucleon polarisation will be zero as shown in equation 2). The extraction will require correcting the experimental azimuthal distribution for angular variations in the acceptance of the nucleon polarimeter from a GEANT simulation.

We can access further polarisation observables utilising the polarised photon beam capabilities at MAMI in conjuncion with our nucleon polarimeter. These observables give the polarisation transferred to the proton from the photon. Forming asymmetries from the different beam polarisations will cancel the acceptances of the nucleon polarimeter. The circular polarised beam-recoil observable $C_{x'}$ can be measured from the azimuthal asymmetry:

$$\frac{N^+(\phi_p') - N^-(\phi_p')}{N^+(\phi_p') + N^-(\phi_p')} = C_{x'}P_\gamma^{circ}A\sin\phi_p' \quad (3)$$

where the $\pm$ refers to the helicity of the beam and A is the analysing power of the polarimeter. It can be seen from equation 2 that the y-component of nucleon polarisation is insensitive to the helicity of the photon beam.

$O_{x'}$ and T are measured simultaneously using a beam of linearly polarised photons. As seen in eqn. 2 this polarisation rotates with the meson azimuthal angle and in order to extract $O_{x'}$ and T we construct an asymmetry that is a function of both ϕ_m and ϕ_p':

$$\frac{N^\perp(\phi_m,\phi_p') - N^\parallel(\phi_m,\phi_p')}{N^\perp(\phi_m,\phi_p') + N^\parallel(\phi_m,\phi_p')} = AP_\gamma^{lin}\left(O_{x'}\sin 2\phi_m\sin\phi_p' + T\cos 2\phi_m\cos\phi_p'\right) \quad (4)$$

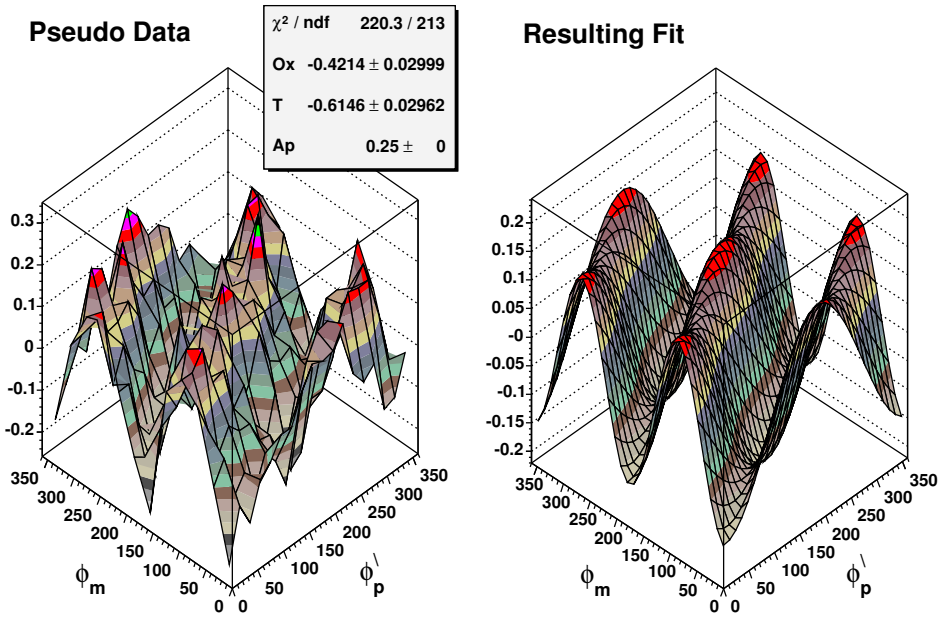

Figure 7: Plots illustrating the technique for extraction of $O_{x'}$ and T. The left hand panel shows pseudo-data created according to eqn. 4 with statistics typically expected in the experiment for a θ_{meson} bin of $\pm 10^{\circ}$ and E_{γ} bin of 25 MeV with the parameters $O_{x'} = -0.4$, $T = -0.6$ and $AP_{\gamma}^{lin} = 0.25$. ϕ_m is the azimuthal angle of the meson and ϕ'_p is the azimuthal scattering angle of the proton in the polarimeter. The right hand panel shows the result of a 2D fit to this pseudo data. The expected errors in the extraction of $O_{x'}$ and T are shown by the errors in the fitted parameters

where the $\parallel$, $\perp$ refer to the direction of linear polarisation. We tested the extraction technique for a realistic situation by generating pseudo-data for $N\left(\phi_m, \phi'_p\right)$ according to eqn. 4 with realistic experimental statistics and parameters described in the caption. With a 2-D fit the input parameters are recovered with errors consistent with those obtained from the error estimate formula $\Delta P_p \sim \frac{2}{\sqrt{(A^2 N)}}$ used in section 5.

4 Count rate estimate and beam time request

The measurement of $C_{x'}$, $O_{x'}$, T and P will be obtained in the same experiment using a photon beam which has both circular and linear polarisation. To obtain high linear and circular beam polarisation over a wide range of photon energies we will carry out two experiments with electron beam energies of 0.85 and 1.5 GeV.

We estimate the beam time required to obtain adequate statistics for double-polarisation observables in both π and η photoproduction in an E_{γ} bin of 25 MeV and a θ_{meson} bin of $\pm 10^{\circ}$. The expected statistical errors are shown in fig. 2 and are outlined more generally below.

The estimate was made using the following input:

- **Tagged photon flux:** A tagged photon rate of $2.5{\times}10^5$ $\gamma s^{-1} MeV^{-1}$.
- **Target:** The liquid hydrogen target is assumed to contain $2.1{\times}10^{23}$ nuclei/cm^2

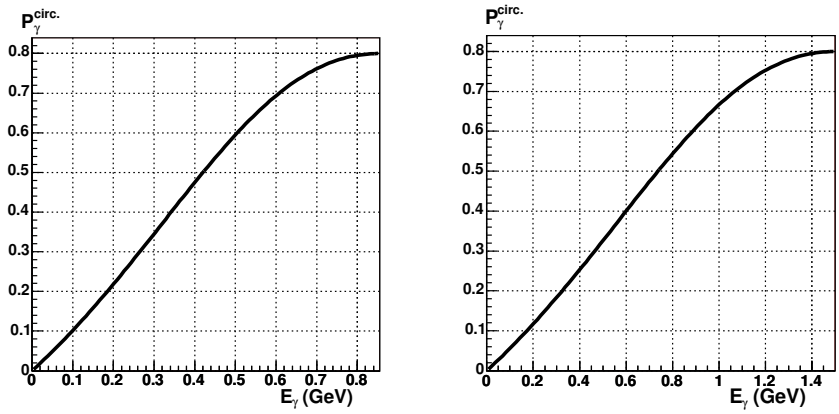

Figure 8: Degree of circular polarisation for the MAMI photon beam with 885 MeV incidenet electron energy (LEFT) and 1.5 GeV (RIGHT)

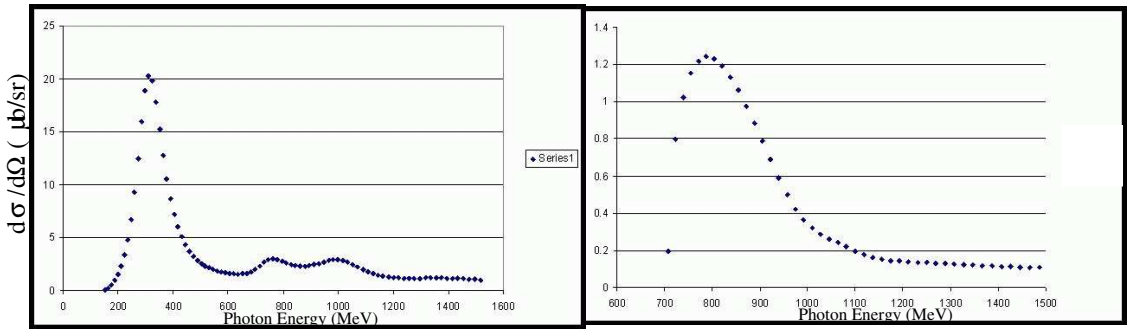

Figure 9: Maid predictions of the cross sections versus incident photon energy for $p(\gamma,p)\pi^0$ (LEFT) and $p(\gamma,p)\eta$ (RIGHT) at a meson CM breakup angle of 135 degrees

- **Cross sections:** For estimates of the typical typical meson photoproduction cross sections we use the MAID paramaterisation. The cross sections at backward meson angles for both p$(\gamma, N)\pi$ and p$(\gamma, N)\eta$ are shown in Fig. 9.
- **Meson detection efficiencies:** A value of ϵ_{meson}=80% was taken for π° and ϵ_{meson}=35% for η detection
- **Data acquisition system live time:** ϵ_{DA} **~70%**
- **Nucleon Polarimeter characteristics:** The probability for a "useful" nucleon scatter in the graphite with angles between 10-30° is taken to be 3%. The average analysing power for the polarimeter is taken to be 0.4.
- **Recoil nucleon count rate:** Therefore the number of usefully scattered nucleons incident on the polarimeter with a θ_{meson} bin of ±10° having typical solid angle Ω_{avg} of 1 sr. and a photon energy bin of width 25 MeV in a beamtime of t seconds is given by :

  $N_{nucleons} = 0.02 \times 2.5{\times}10^5 \times 25 \times 2.1{\times}10^{23} \times \sigma_{avg} \times \Omega_{avg} \times \epsilon_{meson} \times \epsilon_{DA} \times t$
- **Accuracy of $\mathbf{C}_{x'}$** The absolute statistical error in the polarisation observables can be determined from the formula $\Delta C_{x'} \sim \sqrt{(\frac{2}{A^2 N})}$ where A is the product of the analysing power of the polarimeter and the degree of circular polarisation of the beam and N is the number of usefully scattered nucleons incident on the polarimeter. Results are shown in the Table.
- **Accuracy of $\mathbf{O}_{x'}$:** Absolute statistical error obtained from the formula $\Delta O_{x'} \sim \frac{2}{\sqrt{(A^2 N)}}$ where A is the product of the analysing power of the polarimeter and the degree of linear polarisation of the beam. This error also applies to the extraction of the single polarisation observable T. Results are shown in the table.

	Beam time	σ_{avg}	$N_{nucleons}$	$\vec{P}^{linear}$	$\vec{P}^{circ}$	$\Delta O_{x'}$	$\Delta C_{x'}$
E_e= 885 MeV $p(\gamma,p)\pi^0$	300 hrs	3(μb/sr)	7.14×10^4	E_γ=300-500: 0.4	E_γ=200-800: 0.5	0.05	0.03
E_e=885 MeV $p(\gamma,p)\eta$	300 hrs	0.7(μb/sr)	0.73×10^4		E_γ=700-800: 0.75		0.06
E_e= 1500 MeV $p(\gamma,p)\pi^0$	500 hrs	1(μb/sr)	4.0×10^4	E_γ=600 -800: 0.4	E_γ=500 -1500: 0.65	0.06	0.03
E_e= 1500 MeV $p(\gamma,p)\eta$	500 hrs	0.2(μb/sr)	0.35×10^4	E_γ=600 -800: 0.4	E_γ=700-1500: 0.65	0.21	0.09

Total Production beam time - 300 hrs with E_e=885 MeV and 500 hrs with E_e=1500 MeV

We would also require beamtime to commission the nucleon polarimeter before the main production run. From the estimates above, a test beamtime of 100 hours would give sufficient statistics to establish the polarimeter capabilities and optimise the design.

Nucleon polarimeter commissioning beam time - 100 hrs

5 Possible future developments

Obviously there are natural extensions of the recoil polarimetry programme proposed here. We will attempt to also measure the observables for the $p(\gamma, n)\pi^+$ reaction from the data we obtain. The success will depend on the π^+ detection capabilities of the CB and will involve estimating the analysing power for neutrons in the graphite.

Measurements of $C_{x'}$ and $O_{x'}$ on the neutron would give valuable complementary information to the proton target data. However the Fermi motion of the neutron in the target will make the kinematic reconstruction of the 4-vector of the recoiling nucleon into the polarimeter difficult. For charged recoils we will investigate possible tracking solutions e.g. development of the MIDAS[9] Si strip tracking detector. For neutron recoils we will investigate possibilities to detect (n,p) events in the analyser with a segmented plastic scintillator or scintillating fibre detector on the downstream face of the graphite, or to use an active plastic scintillator scatterer.

The polarimeter may also be of great utility in measurements of 2π photoproduction reactions which have sizable cross sections in the energies accessible at MAMI-C. Test data to establish the feasibility of this will be obtained from the proposed measurement.

In the longer term we will also investigate possibilities for target-recoil measurements, the feasibility of which will likely depend on the limitations of the achievable photon flux imposed by the new polarised target system at MAMI.

References

[1] F.X. lee *et. al.*, hep-lat/0208070

[2] T.D. Cohen and L.Y. Glozman, Int. Journ. Mod. Phys. A17, 1327 (2002)

[3] Guy F. de Teramond and Stanley J. Brodsky, Phys. Rev. Lett. 94, 201601 (2005)

[4] J. Ahrens *it. al.*, Phys. Rev. Lett. 88, 232002 (2002)

[5] D. Dutta, H. Gao and T-S H Lee, Phys. Rev. C 65 (2002) 044619;

[6] K. Wijesooriya *et. al.*, Phys. Rev. C 66 (2002) 034614;

[7] A. Bock *et. al.*, Phys. Rev. Lett. 81, 534?537 (1998)

[8] J.Ajaka *et. al.*, Phys. Rev. Lett. 81, 1797?1800 (1998)

[9] S. Altieri *et. al.*, NIM A452 195 (2000)

[10] G. Audit *et. al.*, Nucl. Instr. and Meth. **A301**, 473(1991).

[11] D.P. Watts, Crystal Ball collaboration meeting, www.physics.gla.ac.uk/~dwatts/pid.html (2003)

[12] R. Novotny, IEEE Trans. Nucl. Sci. A **38**, 379 (1991).

[13] Th. Pospischil *et. al.*, Nucl. Inst. and Meth. A 483 (2002) 713.